Ground-state spin logic

J. D. WHITFIELD[1,2,3(a)], M. FACCIN[2(b)] and J. D. BIAMONTE[2,4(c)]

[1] *Department of Physics, Columbia University - 538 W. 120th St, New York, NY 10027, USA*
[2] *Institute for Scientific Interchange - Via Alassio 11/c, 10126 Torino, Italy, EU*
[3] *Quantum Information Technologies, NEC Laboratories America - 4 Independence Way, Princeton, NJ 08540, USA*
[4] *Centre for Quantum Technologies, National University of Singapore - Block S15, 3 Science Drive 2,
Singapore 117543*

Abstract – Designing and optimizing cost functions and energy landscapes is a problem encountered in many fields of science and engineering. These landscapes and cost functions can be embedded and annealed in experimentally controllable spin Hamiltonians. Using an approach based on group theory and symmetries, we examine the embedding of Boolean logic gates into the ground-state subspace of such spin systems. We describe parameterized families of diagonal Hamiltonians and symmetry operations which preserve the ground-state subspace encoding the truth tables of Boolean formulas. The ground-state embeddings of adder circuits are used to illustrate how gates are combined and simplified using symmetry. Our work is relevant for experimental demonstrations of ground-state embeddings found in both classical optimization as well as adiabatic quantum optimization.

The embedding of energy landscapes into the ground-state subspace of spin systems is a task commonly encountered in both classical [1–3] and quantum optimization [4–6]. Finding a state in this subspace is equivalent to a wide variety of NP-complete decision problems and NP-hard optimization problems [1,2,7–10] which have received renewed interest in the wake of adiabatic quantum computation [4,11–15] and its experimental realizations [16–22]. While using quantum resources does not change the intrinsic computational complexity of a problem, it is hoped that quantum annealing offers a polynomial improvement over classical schemes for some NP-hard problems. Recent works have focused on embedding cost functions into the ground-state subspace of spin systems [5,9,11–15,23–29] and cellular automata [25,30–32]. While the emphasis and techniques used in previous work varies, many of the fundamental results overlap.

In this letter, we use symmetries of Boolean functions to unify and extend various constructions of Hamiltonians embedding Boolean functions into their ground-state subspaces. We perform a systematic analysis of the Hamiltonians embedding all two-input, one-output gates using our group-theoretic approach. We also report our new family of Hamiltonians embedding the universal logic gate NAND and present a new XOR Hamiltonian embedding which encompass several previous results [23,24,29]. Both of our constructions have three free parameters providing previously ignored degrees of freedom which could be useful when considering experimental constraints. Extensions of our symmetry arguments to larger Boolean functions are demonstrated using adder circuits of increasing complexity.

While we focus on embedding circuits into the ground state, the application of symmetry arguments is quite general and can be used in the construction of Hamiltonians for other embedding problems recently studied in adiabatic quantum computing such as lattice protein folding [28,33], adiabatic quantum simulation [34], machine learning [27], or search engine rankings [26].

Throughout this letter, we use diagonal Hamiltonians of N spins

$$H = \sum_i c_i \sigma_i + \sum_{ij} c_{ij} \sigma_i \sigma_j + \sum_{ijk} c_{ijk} \sigma_i \sigma_j \sigma_k + \dots \quad (1)$$

with $\sigma \equiv \sigma^z$ defined by $\sigma = |0\rangle\langle 0| - |1\rangle\langle 1|$. Since the eigenvalues of σ are ± 1, we identify Boolean variable, $x \in \{0, 1\}$, with $(\mathbf{1} - \sigma)/2$ instead of σ itself. The subscript of each σ

(a)Current address: Vienna Center for Quantum Science and Technology - Boltzmanngasse 5, 1090 Vienna, Austria, EU; E-mail: james.whitfield@univie.ac.at; jdwhitfield@gmail.com
(b)E-mail: mauro.faccin@isi.it
(c)E-mail: jacob.biamonte@qubit.org

indicates which spin the operator acts on. Terms such as $\sigma_i\sigma_j$ are understood as the tensor product $\sigma_i \otimes \sigma_j$.

Limiting the Hamiltonian in eq. (1) to two-spin interactions yields the experimentally relevant [17,19–22] tunable Ising Hamiltonian which will be our primary focus. Tunable couplings are experimental realized, *e.g.*, through mutual capacitance or shared inductance in super-conducting qubits or, in the case of trapped ions, couplings between ions are induced using off-resonant pairs of lasers or manipulation of vibrational normal modes [19].

The idea of ground-state spin logic is to embed Boolean functions, $f\colon \{0,1\}^n \to \{0,1\}^m$, into the ground-state subspace, $\mathcal{L}(H_{f(\mathbf{x})})$, of spin Hamiltonian $H_{f(\mathbf{x})}(\sigma_i, \sigma_j, \cdots, \sigma_k)$ acting on the spins σ_i, σ_j, ..., σ_k. As an example, consider the universal NAND gate: $\bar{x} \vee \bar{y} = \overline{x \wedge y}$. Here and throughout, for Boolean variables x and y: $\bar{x}$ is the negation of variable x; the logical disjunction (OR), written $x \vee y$, yields the logical one if and only if $x = 1$ or $y = 1$ or both; and the logical conjunction (AND), written $x \wedge y$, evaluates to the logical one if and only if both $x = 1$ and $y = 1$. The corresponding Hamiltonian, $H_{\bar{x} \vee \bar{y}}(\sigma_1, \sigma_2, \sigma_3)$, should have the following ground-state subspace:

$$\begin{aligned}\mathcal{L}(H_{\bar{x} \vee \bar{y}}) &= \mathrm{span}\{|x\rangle|y\rangle|\bar{x} \vee \bar{y}\rangle\} \\ &= \mathrm{span}\{|001\rangle, |011\rangle, |101\rangle, |110\rangle\}. \quad (2)\end{aligned}$$

Using the σ matrices, such a Hamiltonian is given in [25] as[1]

$$H_{\bar{x} \vee \bar{y}}(\sigma_1, \sigma_2, \sigma_3) = 2\mathbf{1} + (\mathbf{1} + \sigma_1 + \sigma_2 - \sigma_1\sigma_2)\,\sigma_3. \quad (3)$$

This construction uses a three-spin interaction which can be replaced using the same number of spins and only two-spin interactions. This was done in [23,24] by penalizing and rewarding certain interactions such that the ground-state subspace is not altered while the higher energy eigenstates are.

Now we introduce the first result of our paper: a three-parameter family of spin Hamiltonians which embed the NAND gate in the ground state using only two-spin interactions. This construction generalizes and subsumes previous gate characterizations found in [23,24,29] and elsewhere. Using coefficients labeled as in eq. (1), the constraint that one eigen-subspace is four-fold degenerate and contains states $|001\rangle$, $|011\rangle$, $|101\rangle$, and $|110\rangle$ leads to the following three equalities:

$$E_{001} = E_{110} \Rightarrow c_3 = c_1 + c_2, \quad (4)$$

$$E_{001} = E_{101} \Rightarrow c_{23} = c_{12} + c_2, \quad (5)$$

$$E_{001} = E_{110} \Rightarrow c_{13} = c_{12} + c_1. \quad (6)$$

---

[1] More precisely, the Hamiltonian found in [25] was given in binary variables as $\Delta(1 - x_C - x_A x_B + x_A x_B x_C)$. Conversion to eq. (3) is done by inserting $(1 - \sigma_i)/2$ for x_i and selecting the appropriate rescaling of Δ.

After enforcing these constraints and utilizing eq. (1), the energies are

$$E_{degen} = E_{001} = -c_1 - c_2 - c_{12}, \quad (7)$$

$$E_{000} = 3(c_1 + c_2 + c_{12}), \quad (8)$$

$$E_{010} = 3c_1 - c_2 - c_{12}, \quad (9)$$

$$E_{100} = 3c_2 - c_1 - c_{12}, \quad (10)$$

$$E_{111} = 3c_{12} - c_1 - c_2. \quad (11)$$

For c_1, c_2, and c_{12} greater than zero, the degenerate space is always the ground state. In closed form, the three-parameter family of Hamiltonians encoding NAND in the ground state is

$$\begin{aligned}H_{\bar{x} \vee \bar{y}}(\sigma_1, \sigma_2, \sigma_3) = {}& (c_1\sigma_1 + c_2\sigma_2)(\mathbf{1} + \sigma_3) \\ & + (c_1 + c_2)\sigma_3 + c_{12} \sum_{i<j} \sigma_i\sigma_j \quad (12)\end{aligned}$$

with $c_1, c_2, c_{12} > 0$. The freedom to select these parameters could be desirable as it reduces the constraints placed on an experimental realization.

The ground-state energy of the NAND Hamiltonian, is $-(c_1 + c_2 + c_{12})$ instead of zero. Some authors choose to consider positive semi-definite Hamiltonians, however the addition of multiples of the identity does not alter energy differences within the landscape of the problem and we choose not to enforce this constraint.

Let us turn to an illustration that shows how to use the Hamiltonian in eq. (12) to construct more complex functions. Naively, it may seem a separate spin must be included for each wire originating from a FANOUT operation [23–25]. However, this is not the case; instead the same spin may be used for the input to as many gates as desired. As an example, in fig. 1, an all-NAND half adder circuit is converted to a spin Hamiltonian using eq. (12). We will return to this example at the end of the letter as an application of our symmetry considerations.

An important consideration for this model is the input and output of the circuit. To extract data from this system, single spin projective measurements can be used. Inputs are set using an additional Hamiltonian

$$H_{in} = \frac{1}{2} \sum_{k}^{inputs} (\mathbf{1} + (-1)^{1-x_k}\sigma_k), \quad (13)$$

which forces the k-th bit to take the value $x_k \in \{0, 1\}$.

There are certain symmetries of Boolean functions from which we can infer properties of the class of Hamiltonians that have the Boolean function embedded in the ground-state subspace. Using group theory to classify Boolean functions is not new [35,36], however, this is its first application to spin system ground-state embeddings.

To limit the scope of our initial discussions, we will restrict our attention to Hamiltonians containing only two-spin interactions and to the set of the 16 two-input, one-output gates.
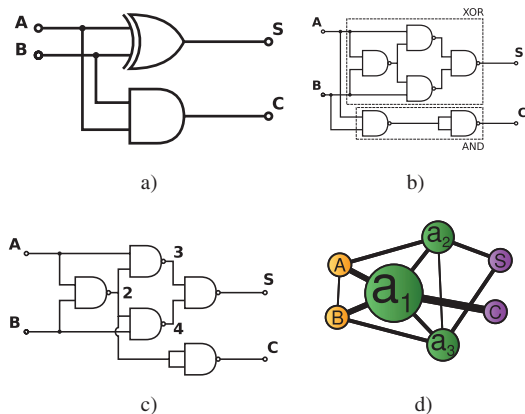
Fig. 1: (Color online) Ground-state embedding of the half adder circuit. (a) The half adder is implemented with a XOR gate and an AND gate. (b) The XOR and AND gates have been substituted by the corresponding all-NAND circuits. (c) The same circuit has been rewritten without the redundant gates and labeled wires. (d) Here the circuit is mapped to a network of seven spins, each corresponding to the seven wires of the circuit. The thickness of each link is proportional to the two-spin interaction strength, while the size of each node is proportional to the local field strength in the two-local reduction. The parameters used for the NAND gate Hamiltonian given in eq. (12) are $c_1 = c_2 = c_{12} = 1$.

Each of the two-input, one-output gates is defined by its truth table:

x	y	z
0	0	b_1
0	1	b_2
1	0	b_3
1	1	b_4

with $b_i \in \{0, 1\}$. There are 16 choices for the vector $b = [b_1, b_2, b_3, b_4]$. The corresponding Hamiltonian, H_b, must have ground-state subspace $\mathcal{L}(H_b) = \{|00b_1\rangle, |01b_2\rangle, |10b_3\rangle, |11b_4\rangle\}$. Thus, there are 16 relevant ground-state subspaces, each corresponding to one of the truth tables.

The symmetry operations on truth tables must treat the output bit differently in order to remain in the space of the 16 truth tables. Thus, we consider i) bit flips of any of the spins and ii) swaps of the two inputs giving the following symmetries: $\{e, F_1, F_2, F_3, R_{12}\}$. Here e is the identity operation, F_i is the spin-flip operation (negate), and R_{12} is the spin-swap operator (permute). The action of the latter two operations on spins is defined via

$$F_i \circ \sigma_j = (1 - 2\delta_{ij})\sigma_j, \tag{14}$$

$$R_{ij} \circ \sigma_k = \sigma_j \delta_{ki} + \sigma_i \delta_{kj} + \sigma_k (1 - \delta_{ki} - \delta_{kj}). \tag{15}$$

The group G can be presented as $G = \langle R_{12}, F_1, F_3 \rangle$ where $\langle \cdot \rangle$ indicates a set of generators. Defining relations of
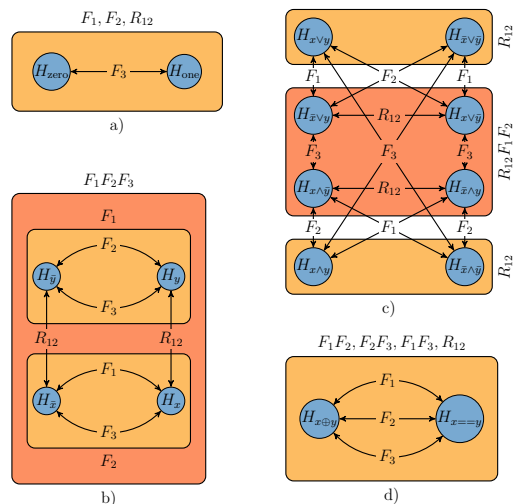

Fig. 2: (Color online) The action of $D_4 \times Z_2$ on the 16 Hamiltonians corresponding to truth tables of two-input, one-output functions. The Hamiltonians can be converted to any other Hamiltonian in the same orbit by applying the spin-flip (negate) F_i or input-swap (permute) R_{12} operations. The symmetry operations that leave the ground-state subspaces of each Hamiltonian invariant (the stabilizer subgroup) is written on the perimeter of each rectangular region. Orbits (a), (b), (c), (d) are explained separately in the text. Each of these orbits requires an additional spin for a Hamiltonian embedding using only two-spin interactions: orbit (a) requires a single spin, (b) two spins, (c) three spins, and orbit (d) requires four spins.

the group are $R_{12}^2 = F_1^2 = F_3^2 = e$, $R_{12}F_1 = F_2 R_{12}$, $F_1 F_3 = F_3 F_1$ and $R_{12}F_3 = F_3 R_{12}$. From these relations, or alternatively from the cycle graph, the group is of order 16 and is isomorphic to $D_4 \times Z_2$, where D_4 is the symmetry group of the square and Z_2 is the cyclic group of order 2.

The action of G on the set of 16 truth tables is depicted in fig. 2. Four orbits are found under action of the group:

$$\{0, 1\},$$
$$\{x, y, \bar{x}, \bar{y}\},$$
$$\{x \vee y, \bar{x} \vee y, x \vee \bar{y}, \cdots, \bar{x} \wedge \bar{y}\},$$
$$\{x \oplus y, x == y\}.$$

These classes are depicted in fig. 2(a), (b), (c), (d), respectively. These classes correspond to different NPN (negate-permute-negate) classes [35,36]. Interestingly, each orbit requires a different number of spins to implement when considering only two-spin interactions. We examine each in turn.

First, consider the constant functions with $b_i = c$ and $c \in \{0, 1\}$. Since these functions do not depend on x nor y, there is no need to couple either to the third spin. Hence, the Hamiltonian in eq. (13) can be used. According to the group action depicted in fig. 2(a), given the Hamiltonian for H_{zero} corresponding to $b_i = 0$, the action of F_3 transforms H_{zero} to H_{one}.

Second, for each of the functions, $b_i = x$, $b_i = y$, $b_i = \bar{x}$ and $b_i = \bar{y}$, the output bit only depends on one of the two inputs. The other input is extraneous, so the gate only requires two spins to implement. The truth tables can be embedded using variations of the COPY gate previously introduced in [23–25]. The general k-COPY gate forces k bits to take the same value and the corresponding diagonal operator

$$H_{k\text{-COPY}} = -\frac{1}{2} \sum_{i \neq j} \sigma_i \sigma_j \qquad (16)$$

acting on k-spins possesses a ground-state subspace $\mathcal{L}(H_{k\text{-COPY}}) = \text{span}\{|0\rangle^{\otimes k}, |1\rangle^{\otimes k}\}$. If we are concerned with constructing a Hamiltonian using a physical set of spins, the spatial locality could play an important role as coupling of distant spins may not be possible. In this case, the k-COPY gate could be useful for spatially distributing intermediate results of the computation. The action of F_1 or F_3 transforms $H_x = H_{2\text{-COPY}(x,z)}$ into the Hamiltonian $H_{\bar{x}}$, as shown in fig. 2(b).

The third class of functions to be considered is $x \vee y$, $x \wedge y$ and all possible negations of the two inputs. Our general formula for $\bar{x} \vee \bar{y}$ is given in eq. (12) and using the symmetry operations from group G, see fig. 2(c), all other gates in this orbit can be derived using three spins with two-spin interaction terms.

The last orbit of functions contains XOR and EQUIV. The XOR of inputs x and y, $x \oplus y$, outputs logical one only when exactly one of the two inputs is one. The EQUIV ($x == y$) outputs logical one only when both inputs have the same value. Neither of these two functions can be embedded in the ground-state subspace of a three-spin system using only two-spin interactions; it requires a fourth ancilla spin to implement using only pairwise interactions. If restricted to three spins, the gate XOR($\oplus$) requires a three-spin interaction.

$$H_{x \oplus y}(\sigma_1, \sigma_2, \sigma_3) = -\sigma_1 \sigma_2 \sigma_3. \qquad (17)$$

The inability to create this operator acting on three spins with two-spin interactions can be demonstrated algebraically or graphically using Karnaugh maps [23,29]. For XOR, the stabilizer subgroup is generated by $F_i F_j$ and R_{12}, see fig. 2(d). When considering the ancilla spin, σ_4, there is an additional F_4 symmetry that leaves the truth table unchanged.

Beginning with the swap-symmetric operators $M_z = \sum_i \sigma_i$ and $M_{zz} = \sum_{i<j} \sigma_i \sigma_j$, we write the most general swap-symmetric Hamiltonian over four spins restricted to two-spin interactions as

$$H_R = r_z M_z + r_{zz} M_{zz} + \sigma_4 (r_4 + r_{z4} M_z). \qquad (18)$$

Suppose that the coefficient vector $R = [r_z, r_{zz}, r_4, r_{z4}]$ gives a valid XOR Hamiltonian. Then we can act with F_4 to get a second Hamiltonian that also preserves the ground-state subspace with coefficients $R' = [r_z, r_{zz}, -r_4, -r_{z4}]$. In refs. [23] and [24], this F_4 symmetry connects the decompositions given as $R = [1, -1, -2, 2]$ and $R = [1, -1, 2, -2]$

in the respective papers. Furthermore, since the ground-state subspace is symmetric with respect to $F_i F_j$, there are an additional six Hamiltonians with logically equivalent ground-state subspaces. For example, beginning with $H_{x \oplus y}$ corresponding to $R = [1, -1, -2, 2]$ and using symmetry operation $F_1 F_2$ results in

$$\begin{aligned} F_1 F_2 \circ H_{x \oplus y} = {} & 2\sigma_4(-\sigma_1 - \sigma_2 + \sigma_3) \\ & + \sigma_1 + \sigma_2 - \sigma_3 - 2\sigma_4 \\ & + (\sigma_1 \sigma_2 - \sigma_2 \sigma_3 - \sigma_1 \sigma_3) \end{aligned} \qquad (19)$$

with the same ground-state subspace. Note that this Hamiltonian is not of the same form as eq. (18) like those given in [23,24].

To extend the XOR Hamiltonians previously listed to a parameterized family of Hamiltonians, we rearrange eq. (18) with $R = [1, -1, -2, 2]$ as

$$\begin{aligned} H_{x \oplus y} = {} & -(\sigma_1 + \sigma_2)(\mathbf{1} - \sigma_4) \\ & - 2\sigma_4 + (\sigma_1 \sigma_2 + \sigma_1 \sigma_4 + \sigma_2 \sigma_4) \\ & - \sigma_3 + \sigma_1 \sigma_3 + \sigma_2 \sigma_3 + 2\sigma_3 \sigma_4. \end{aligned} \qquad (20)$$

Comparing with eq. (12) and using fig. 2c, we can simplify this equation using $H_{\bar{x} \wedge \bar{y}}(\sigma_1, \sigma_2, \sigma_4) = F_1 F_2 F_4 \circ H_{\bar{x} \vee \bar{y}}(\sigma_1, \sigma_2, \sigma_4)$ evaluated at $c_1 = c_2 = c_{12} = 1$. Generalizing to other values of c_1, c_2, and c_{12}, we arrive at the following three-parameter family that preserves the ground-state subspace of XOR:

$$\begin{aligned} H_{x \oplus y} = {} & H_{\bar{x} \wedge \bar{y}}(\sigma_1, \sigma_2, \sigma_4) - \sigma_3 \\ & + \sigma_1 \sigma_3 + \sigma_2 \sigma_3 + 2\sigma_3 \sigma_4. \end{aligned} \qquad (21)$$

By examining the excited state structure of eq. (20), we find that in the parameterization of $H_{\bar{x} \wedge \bar{y}}$ the coefficients, c_1, c_2, c_{12}, must be greater than $1/2$ instead of strictly positive.

Our work has direct relevance to recent experimental realizations of adiabatic quantum annealing in superconducting qubits [21,22] and ion traps [16–20]. At the start of the adiabatic computation, the initial Hamiltonian is usually chosen as a sum of transverse local magnetic fields while at the end of the evolution the Hamiltonian encodes problem instances in its ground state in the Ising basis. Our results provide a symmetry-based classification of logically equivalent Hamiltonians as well as providing unifying formulas for Boolean embeddings.

In table 1, we summarize our results for Hamiltonian embeddings of two-input, one-output Boolean functions. While we have restricted attention to diagonal Hamiltonians, future work could consider transformations where the ground state is preserved but the Hamiltonian obtains off-diagonal elements.

Now we return to the half adder example from fig. 1. With our constructions, we can directly implement it using the XOR and AND gates,

$$H_{HA} = H_{x \oplus y}(\sigma_A, \sigma_B, \sigma_a, \sigma_S) + H_{x \wedge y}(\sigma_A, \sigma_B, \sigma_C). \qquad (22)$$

Table 1: Summary of representative Hamiltonians from each orbit under the action of the symmetry group. Spin one and two correspond to the two inputs while spin three corresponds to the output. The fourth spin is an ancilla spin needed only for the implementation of XOR and EQUIV. In the AND, OR, ..., NAND, NOR family, the sign of the coefficients determines which gate on this NPN orbit one obtains. We have only shown four Hamiltonians and the remaining 12 Hamiltonians as well as additional Hamiltonians with different excited states are related via the action of the group $D_4 \times Z_2$ as depicted in fig. 2.

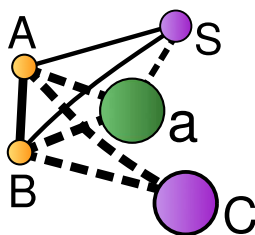| $z = f(x,y)$	$H_{f(x,y)}(\sigma_1, \sigma_2, \sigma_3, \sigma_4)$
Constant functions	
$z = 0$	$H_{zero} = (\mathbf{1} - \sigma_3)$
Copy-type functions	
$z = x$	$H_x = (\mathbf{1} - \sigma_1 \sigma_3)$
AND, OR, ..., NAND, NOR functions	
$z = \bar{x} \vee \bar{y}$	$H_{\bar{x} \vee \bar{y}} = (c_1\sigma_1 + c_2\sigma_2)(\mathbf{1} + \sigma_3)$ $+ (c_1 + c_2)\sigma_3 + c_{12}\sum_{i<j}^{3}\sigma_i\sigma_j$
XOR and EQUIV functions	
$z = x \oplus y$	$H_{x \oplus y} = H_{\bar{x} \wedge \bar{y}}(\sigma_1, \sigma_2, \sigma_4) - \sigma_3$ $+ \sigma_1\sigma_3 + \sigma_2\sigma_3 + 2\sigma_3\sigma_4$

Fig. 3: (Color online) The half adder spin Hamiltonian that arises from the four-spin decomposition of the XOR Hamiltonian which simplifies the construction from fig. 1(d). Dashed links represent negative interactions and checkerboard shading indicates a negative local field. The size of the nodes and the thickness of the edges are proportional to the fields and interaction strength (on spins A and B there is no local field). The parameters used for the AND gate and XOR gate are $c_1 = c_2 = c_{12} = 1$.

Here σ_A and σ_B correspond to the inputs to be summed, σ_a corresponds to the XOR ancilla bit, and σ_S and σ_C correspond to the sum and carry bits. As depicted in fig. 3, the new spin Hamiltonian uses two less ancilla spins than our earlier construction. This is important in computational situations with limited numbers of spins as is frequently the case in experimental quantum annealing. A large equivalence class of Hamiltonians arises from the D_4 stabilizer subgroup of the XOR Hamiltonian and the Z_2 stabilizer subgroup of the AND Hamiltonian.

The symmetry group of H_{HA} can be inferred from the symmetries of the component Hamiltonians using a direct product structure. For a general circuit Hamiltonian composed of gate Hamiltonians acting on subsets of spins, $H = \sum H_i$, the stabilizer subgroup is the direct product of the stabilizers for each of the Hamiltonians in the sum. The direct product group action is defined as $(g_1, g_2, \cdots g_N) \circ$

$H = \sum g_i \circ H_i$. If g is in the intersection of all stabilizer groups (the diagonal subgroup), then $g \circ H$ will have the same ground-state subspace as H.

Additional symmetries arise after partitioning the bits into output and ancilla bits. We can expect the symmetries of the Boolean function being embedded to be possessed by the resulting Hamiltonian. However, the symmetry group composed of the gate-local symmetries preserves the full ground-state subspace including the values of the ancilla bits. The symmetries of the Boolean function before being decomposed into logic gates will arise as global symmetries that cannot be obtained from the gate-local symmetries of the individual gates. For instance, if σ_a corresponds to an ancilla spin, then inverting this bit in each circuit component leaves the ground-state subspace invariant. That is, H and $(F_a, F_a, \cdots, F_a) \circ H$ embed the same Boolean function.

As a further illustration of the distinction between global and gate-local symmetries, consider the full adder corresponding to a Boolean function which adds binary summands A, B, and carry-in bit C_{in}. The permutation of the input bits and the carry-in bit is a symmetry of the full adder Boolean function. However, such a permutation is not a gate-local symmetry of the sub-Hamiltonians used in the circuit embedding. This is because the values of the ancilla spin within the ground-state subspace is not preserved under this permutation. Thus, the local symmetries do not determine all possible symmetries when some bits are considered as ancillas.

As a final example of ground-state spin logic, fig. 4 shows the spin Hamiltonian of the ripple carry adder for four-bit binary numbers. The figure shows the network for both an implementation with only NAND gates in fig. 4(a) and an implementation with XOR, AND, and OR gates in fig. 4(b). As in fig. 1(b) and (c), the larger gate set allows a simpler circuit construction which translates to a spin system with 14 less spins. In general, when adding n-bit numbers, the constructions differ by $4n - 2$ spins. Both of our constructions include parameters which can be freely varied without altering the ground-state allowing for robust implementations. Another salient feature is that the average number of connections per spins increases from 3.85 in the all-NAND case to 4.22. One may opt for the all-NAND construction if a major hurdle is multiple couplings. Explicitly listing the free parameters and the symmetries that preserve the ground-state subspace is an illustration of how our approach gives experimentalists and theorists systematic methods to find additional degrees of freedom and classify logically equivalent Hamiltonians.

An important step towards large scale experimental realizations of the techniques presented in this paper will be the quantum adiabatic implementation and characterization of the elementary logic gates. In the case of XOR, this Hamiltonian will allow one to realize an effective three-spin interaction by using only two-spin interactions and introducing an ancilla spin. Such an interesting example is in line with current experimental capabilities [20–22].
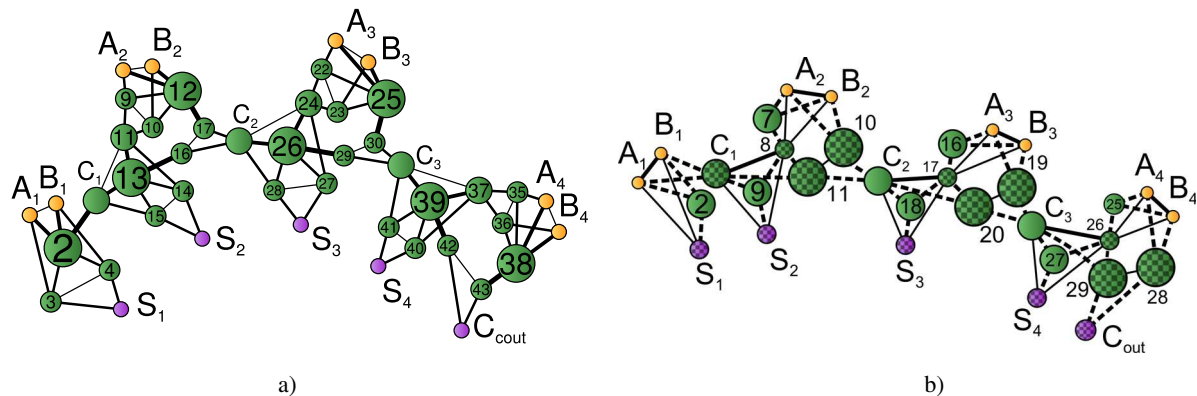
Fig. 4: (Color online) Ripple carry adder. The figure shows the network of spins corresponding to a ripple carry adder with four bits. The ripple carry adder is composed by one half adder and three full adders; in yellow it shows the input spins from the four bits binary numbers $A = \sum_{i=1}^{4} A_i 2^i$ and $B = \sum_{i=1}^{4} B_i 2^i$; while the sum spins, S_i are drawn in purple. Carry bits are labeled as C_i. The direction of the sum is from left to right. Panel (a) shows a ripple carry constructed with only NAND gates and parameters $c_1 = c_2 = c_{12} = 1$, while (b) shows the same adders built with XOR, AND and OR gates.

REFERENCES

[1] HARTMANN A. K. and WEIGT M., *Phase Transitions in Combinatorial Optimization Problems* (Wiley-VCH) 2005.
[2] BARAHONA F., *J. Phys. A: Math. Gen.*, **15** (1982) 3241.
[3] KIRKPATRICK S., GELATT C. D. and VECCHI M. P., *Science*, **220** (1983) 671.
[4] OHZEKI M. and NISHIMORI H., *J. Comput. Theor. Nanosci.*, **8** (2011) 963.
[5] DAS A. and CHAKRABARTI B. K., *Rev. Mod. Phys.*, **80** (2008) 1061.
[6] DAS A. and CHAKRABARTI B. K. (Editors), *Quantum Annealing and Related Optimization Methods* (Springer) 2005.
[7] ALTSHULER B., KROVI H. and ROLAND J., arXiv:0908.2782 (2009).
[8] ALTSHULER B., KROVI H. and ROLAND J., *Proc. Natl. Acad. Sci. U.S.A.*, **107** (2010) 12446.
[9] CHOI V., *Quantum Inf. Commun.*, **11** (2011) 0638.
[10] DICKSON N. and AMIN M. H. S., *Phys. Rev. Lett.*, **106** (2011) 050502.
[11] APOLLONI B., CARAVALHO N. and FALCO D. D., *Quantum Stoch. Optim.*, **33** (1989) 233.
[12] AMARA P., HSU D. and STRAUB J. E., *J. Phys. Chem.*, **97** (1993) 6715.
[13] FINNILA A. B., GOMEZ M. A., SEBENIK C., STENSON C. and DOLL J. D., *Chem. Phys. Lett.*, **219** (1994) 343.
[14] KADOWAKI T. and NISHIMORI H., *Phys. Rev. E*, **58** (1998) 5355.
[15] FARHI E., GOLDSTONE J., LAPAN J., LUNDGREN A. and PREDA D., *Science*, **292** (2001) 472.

[16] FRIEDENAUER A., SCHMITZ H., GLUECKERT J. T., PORRAS D. and SCHAETZ T., *Nat. Phys.*, **4** (2009) 757.
[17] KIM K. *et al.*, *Nature*, **465** (2010) 590.
[18] ISLAM R. *et al.*, *Nat. Comm.*, **2** (2011) 377.
[19] KIM K. *et al.*, *New J. Phys.*, **13** (2011) 105003.
[20] BRITTON J. W. *et al.*, *Nature*, **484** (2012) 489.
[21] JOHNSON M. W. *et al.*, *Nature*, **473** (2011) 194.
[22] HARRIS R. *et al.*, *Phys. Rev. B*, **82** (2010) 024511.
[23] BIAMONTE J. D., *Phys. Rev. A*, **77** (2008) 052331.
[24] GU M. and PERALES A., *Phys. Rev. E*, **86** (2012) 011116.
[25] CROSSON I. J., BACON D. and BROWN K. R., *Phys. Rev. E*, **82** (2010) 031106.
[26] GARNERONE S., ZANARDI P. and LIDAR D. A., *Phys. Rev. Lett.*, **108** (2012) 230506.
[27] PUDENZ K. L. and LIDAR D. A., arXiv:1109.0325 (2011).
[28] PERDOMO A., TRUNCIK C., TUBERT-BROHMAN I., ROSE G. and ASPURU-GUZIK A., *Phys. Rev. A*, **78** (2008) 012320.
[29] ROSENBAUM D. and PERKOWSKI M., in *IEEE, International Symposium on Multiple-Valued Logic*, edited by ESTEVA F., GISPERT J. and MANYÀ F. (IEEE Computer Society, Washington, DC) 2010, p. 270.
[30] LENT C. S., TOUGAW P. D. and POROD W., *Quantum cellular automata: The physics of computing with arrays of quantum dot molecules*, in *Proceedings of the Workshop on Physics and Computation* (IEEE Computer Society, Dallas Chapter) 1994, pp. 5–13.
[31] GU M., WEEDBROOK C., PERALES A. and NIELSEN M. A., *Physica D*, **238** (2009) 835.
[32] BURGARTH D., GIOVANNETTI V., HOGBEN L., SEVERINI S. and YOUNG M., arXiv:1106.4403 (2011).
[33] PERDOMO A., DICKSON N., DREW-BROOK M., ROSE G. and ASPURU-GUZIK A., arXiv:1204.5485 (2012).
[34] BIAMONTE J. D., BERGHOLM V., WHITFIELD J. D., FITZSIMONS J. and ASPURU-GUZIK A., *AIP Adv.*, **1** (2011) 022126.
[35] CORREIA V. P. and REIS A. I., *Classifying n-input Boolean functions*, in *Proceedings of the VII Workshop Iberchip* (2001) p. 58, see Session 10 of http://www.iberchip.net/VII/cdnav/cd_home.htm.
[36] CHANG C.-H. and FALKOWSKI B. J., *Electron. Lett.*, **10** (1999) 798.